Investigation of the use of density functional in second- and third-row transition metal dimer calculations

ARTICLE *in* JOURNAL OF COMPUTATIONAL CHEMISTRY · DECEMBER 2001

Impact Factor: 3.59 · DOI: 10.1002/jcc.1148 · Source: DBLP

3 AUTHORS, INCLUDING:

Susumu Yanagisawa
University of the Ryukyus
51 PUBLICATIONS **1,467** CITATIONS

SEE PROFILE

Takao Tsuneda
University of Yamanashi
68 PUBLICATIONS **3,909** CITATIONS

SEE PROFILE

Journal of Theoretical and Computational Chemistry
Vol. 4, No. 1 (2005) 265–280

World Scientific
www.worldscientific.com

INVESTIGATION OF DOMINANT ELECTRON CONFIGURATIONS IN TIME-DEPENDENT DENSITY FUNCTIONAL THEORY

SUSUMU YANAGISAWA, TAKAO TSUNEDA and KIMIHIKO HIRAO

Department of Applied Chemistry, School of Engineering
The University of Tokyo, Tokyo
113-8656, Japan

Received 13 May 2004
Accepted 9 June 2004

We investigated the electron configurations that are dominant in excited states of molecules in time-dependent density functional theory (TDDFT). By taking advantage of the discussion on off-diagonal elements in the TDDFT response matrix (Appel *et al.*, *Phys Rev Lett*, **90**, 043005, 2003), we can pick up electron transitions that contribute to an excitation of interest by making use of the diagonal elements of the TDDFT matrix. We can obtain approximate excitation energies by calculating a TDDFT submatrix, which is contracted for a list of collected transitions. This contracted TDDFT was applied to the calculation of excitation energies of the CO molecule adsorbing Pt_{10} cluster and some prototype small molecules. Calculated results showed that a TDDFT excitation energy is dominated by a few electron configurations, unless severe degeneracy is involved.

Keywords: TDDFT; small matrix approximation; contracted TDDFT submatrix.

1. Introduction

Time-dependent density functional theory (TDDFT)[1–5] has gained widespread use in photochemistry due to its reasonable accuracy even though its computational cost is low. TDDFT has been used to reproduce or to anticipate the experimental electronic spectra of various chemical species: radicals,[5,6] metal oxides,[7–9] carbonyls,[10] aromatics,[11] porphyrins,[12,13] polycyclic aromatic hydrocarbons,[14,15] etc. At present, TDDFT has some deficiencies, specifically in underestimating Rydberg excitation energies[16–19] and in poorly estimating charge-transfer excitations.[20–23] This is probably due to its insuficient long-range interaction in exchange-correlation functionals used. Nevertheless, TDDFT has been accepted as a powerful tool for investigating the photochemistry of large systems: e.g. biomolecules and nanomaterials. Furthermore, analytical gradient of TDDFT excitation energy is available recently,[24–26] which may enable the TDDFT excited state molecular dynamics simulation.

The remarkable accuracy of TDDFT, as was found in the previous calculations,[4–15] can be attributed to its formally exact formulation as a single-excitation theory based on Kohn–Sham orbitals, in which dynamical electron correlation is taken into account. In practice, TDDFT, using current approximate functionals and the adiabatic local density approximation, performs significantly better than the conventional Hartree–Fock (HF)-based single-excitation theories such as configuration interaction with single substitutions (CIS) or random-phase approximation (RPA) for low-lying valence excited states,[4,5] with their computational costs comparable to TDDFT. It was also found that the low-lying valence excitation energies of radicals with the corresponding excited states being of substantial double excitation character are significantly improved by TDDFT over unrestricted CIS or restricted open-shell CIS, even though all of them are single-excitation theories.[5] These results indicate that TDDFT recovers the dynamical correlation that is absent in HF-based single-excitation theories. In other words, the dynamical correlation in TDDFT improves the efficiency of describing electronic excitations. We therefore expect that TDDFT is capable of describing electronic excitations of molecules with smaller number of electron configurations than is expected for HF-based single-excitation theories. This situation is readily confirmed by the solution vectors of excited states obtained in excitation spectra calculations of molecules: the solution vectors of TDDFT are often dominated by a few configurations, in contrast to those of RPA or CIS, which are in general linear combinations of several configurations with comparable weights.[5] This feature may cause the rapid convergence in diagonalization of the TDDFT matrix employing the Davidson's iterative subspace method,[27] which is prevailing in typical TDDFT codes.[4,28–30] There is, however, no investigation of electron configurations that are essentially dominating the excited states of molecules in TDDFT calculations. Appel *et al.* suggested an approach that examines the availability of TDDFT by taking diagonal terms of the TDDFT matrix into account.[31] Using this approach, it is possible to pick up electron configurations that are energetically coupled to the excited states of interest.

In this study, by making use of their approach, we investigate the electron configurations that are dominant in excited states of molecules described by TDDFT. The approach of Appel *et al.* is used for contracting the original TDDFT matrix into the one of smaller rank in which the constituent electron configurations are energetically coupled to the excited state of interest. By solving the eigenvalue equation for this contracted matrix instead of the original full matrix, we demonstrate that TDDFT reproduces the excitation energies of molecules with reasonable accuracy even though only a few dominant electron configurations are taken into account. This information may contribute to the acceleration of the TDDFT investigation that involves a successive calculation of a specific excited state, such as the excited state potential energy surface calculation and a subsequent excited state molecular dynamics simulation. In Sec. 2, we describe the theoretical background of deriving a contracted TDDFT matrix from the original one based on the discussion of

Appel *et al.*[31] In Secs. 3 and 4, we apply this contraction scheme to the excited states of CO adsorbing Pt_{10} cluster and some prototype small molecules and discuss the efficiency and the accuracy of TDDFT. In Sec. 4, we draw our conclusions.

2. Theoretical Background

Let us begin with a brief review of the basic solution of the time-dependent Kohn–Sham (TDKS) method for the sake of better understanding. In TDKS calculations, the square of excitation energies, $\Omega = \omega^2$, is obtained by solving an eigenvalue equation,[4,5,31,32]

$$\sum_{q^0} \Omega_{qq^0} \upsilon_{q^0} = \Omega \upsilon_q, \tag{1}$$

where q is an index that represents a transition from the ith σ-spin occupied Kohn–Sham (KS) orbital, $\phi_{i\sigma}$, to the ath σ-spin unoccupied KS orbital, $\phi_{a\sigma}$. The corresponding oscillator strengths are calculated by using the response function υ_q. The matrix Ω_{qq^0} is expressed by

$$\Omega_{qq^0} = \delta_{qq^0}\Omega_q + 2\sqrt{\omega_q \omega_{q^0}} M_{qq^0}(\omega), \tag{2}$$

where $\omega_q = \epsilon_{a\sigma} - \epsilon_{i\sigma}$ ($\epsilon_{i\sigma}$ is the KS eigenvalue corresponding to $\phi_{i\sigma}$) and

$$M_{qq^0}(\omega) = \int d^3\mathbf{r} \int d^3\mathbf{r}^0 \phi^*_{i\sigma}(\mathbf{r}) \phi_{a\sigma}(\mathbf{r}) f_{HXC}(\mathbf{r}, \mathbf{r}^0, \omega) \phi_{j\sigma^0}(\mathbf{r}^0) \phi^*_{b\sigma^0}(\mathbf{r}^0). \tag{3}$$

In Eq. (3), f_{HXC} is the Hartree-exchange-correlation (HXC) kernel,

$$f_{HXC}(\mathbf{r}, \mathbf{r}^0, \omega) = \frac{1}{|\mathbf{r} - \mathbf{r}^0|} + \frac{\delta^2 E_{XC}[\rho_\alpha, \rho_\beta]}{\delta\rho_\sigma(\mathbf{r}) \delta\rho_{\sigma^0}(\mathbf{r}^0)}, \tag{4}$$

where $\delta^2 E_{XC}/\delta\rho_\sigma \delta\rho_{\sigma^0}$ is the second derivative of an exchange-correlation energy functional that is usually given by using the adiabatic local-density approximation, i.e. $\delta^2 E_{XC}/\delta\rho_\sigma \delta\rho_{\sigma^0}(\mathbf{r}, \mathbf{r}^0, \omega) \cong \delta^2 E_{XC}/\delta\rho_\sigma \delta\rho_{\sigma^0}(\mathbf{r})$.

Appel, Gross, and Burke discussed the accuracies of calculated TDKS excitation energies and oscillator strengths in terms of the electronic structures of systems that have a large difference in degeneracy.[31] In their study, it was stated that accurate TDKS excitation energies could be elucidated by ignoring all off-diagonal terms of M_{qq^0}, i.e. by a small matrix approximation (SMA), where the eigenvalue Ω in Eq. (1) is approximated by the diagonal term,

$$\Omega^{SMA} = \Omega_q + 2\omega_q M_{qq}. \tag{5}$$

This approximation is supported by the fact that M_{qq^0} decays rapidly with distance from the diagonal.[31] The first correction for Ω^{SMA} was given by using a continued-fraction method[33] as a perturbation expansion of the off-diagonal elements to the second order,

$$\Omega = \Omega_q^{SMA} + \sum_{q^0 \neq q} \frac{4\omega_q \omega_{q^0} |M_{qq^0}|^2}{\Omega_q^{SMA} - \Omega_{q^0}^{SMA}}. \tag{6}$$

By defining the shift from the KS value, $\Omega_q = (\epsilon_{a\sigma} - \epsilon_{i\sigma})^2$, as

$$\Delta\Omega_q = \Omega - \Omega_q, \tag{7}$$

Eq. (6) is transformed into

$$\Delta\Omega_q = \Delta\Omega_q^{SMA}\left[1 + \sum_{q^0 \neq q} \frac{\Delta\Omega_{q^0}^{SMA}}{\Omega_q^{SMA} - \Omega_{q^0}^{SMA}} \frac{|M_{qq^0}|^2}{M_{qq}M_{q^0q^0}}\right]. \tag{8}$$

By assuming

$$M_{qq^0} \approx \sqrt{M_{qq}M_{q^0q^0}}, \tag{9}$$

it was suggested that the off-diagonal terms of Ω_{qq^0} in Eq. (2) do not contribute to the calculated TDKS results if these off-diagonal terms satisfy

$$\sum_{q^0 \neq q} \frac{\Delta\Omega_{q^0}^{SMA}}{\Omega_q^{SMA} - \Omega_{q^0}^{SMA}} \ll 1. \tag{10}$$

Following this relation, we concluded that the calculated accurate excitation energies and oscillator strengths in the TDKS may be explained by small off-diagonal matrix elements of M_{qq^0}. It is also presumed that the excitation energies of interest may be approximated with reasonable accuracy by incorporating only a few significant off-diagonal elements.

We make use of Eq. (10) for taking into account only the electron configurations that are dominant in the excited states of interest, i.e. we reduce the off-diagonal elements of M_{qq^0} that are necessary to calculate the excitation energy corresponding to transition q ($\phi_{i\sigma} \rightarrow \phi_{a\sigma}$) while maintaining the quality of the original TDKS calculation. By making use of Eq. (10), we can classify significant transitions $\{q^0\}$ that considerably contribute to the excited states containing transition q. Based on Eq. (10), significant transitions q^0 may satisfy

$$\left|\frac{\Delta\Omega_{q^0}^{SMA}}{\Omega_q^{SMA} - \Omega_{q^0}^{SMA}}\right| = \left|\frac{2\omega_{q^0}M_{q^0q^0}}{\omega_q^2 - \omega_{q^0}^2 + 2(\omega_q M_{qq} - \omega_{q^0}M_{q^0q^0})}\right| > \theta, \tag{11}$$

where θ is a threshold that is arbitrarily given. One should notice that Eq. (11) is expressed by using only the diagonal elements, M_{qq} and $M_{q^0q^0}$, and the energy gaps of KS orbitals, ω_q and ω_{q^0}. We would like to emphasize that Eq. (11) is generally more acceptable than Eq. (10), because this equation is sufficient for the second term in Eq. (8) < 1. We investigate the availability of the approximation of reducing the off-diagonal elements based on Eq. (11) as follows:

(1) The left side of Eq. (11) is calculated by using $\{M_{qq}\}$ and $\{\omega_q\}$.
(2) If the calculated value satisfies Eq. (11), transition q^0 is added to the list of contributable transitions, $\{q^0\}$.
(3) The TDKS eigenvalue equation in Eq. (1) is then solved for the small matrix Ω_{qq^0} in Eq. (2) that is contracted for the listed transitions only.
(4) Steps (1)–(3) are done for each of the irreps.

We perform the TDKS calculation employing a contracted matrix derived with Eq. (11) on various thresholds θ. By calculating the excitation energies approximated by the contracted matrix corresponding to each of the θ's, we can find the electron configurations that are dominant in excited states of interest.

3. Computational Details

With the contraction scheme described in the previous section, we investigated the dominant configurations in excited states obtained by TDKS calculation for CO molecule adsorbing Pt(111) surface and some prototype molecules.

The CO/Pt(111) system has been investigated in several theoretical studies[34,35] and in a UV/HREELS experiment.[34] As shown in Fig. 1, a Pt_{10} cluster model was adopted for the Pt(111) surface, with its interatomic distance set as the experimental one. The adsorption structure of the CO molecule was determined by KS calculations on the DMol^3 program[36–40] with a Becke 1988 exchange[41] plus a one-parameter progressive correlation (BOP) functional[42] using a double numerical with polarization basis functions and an effective core potential (dnp/ecp).

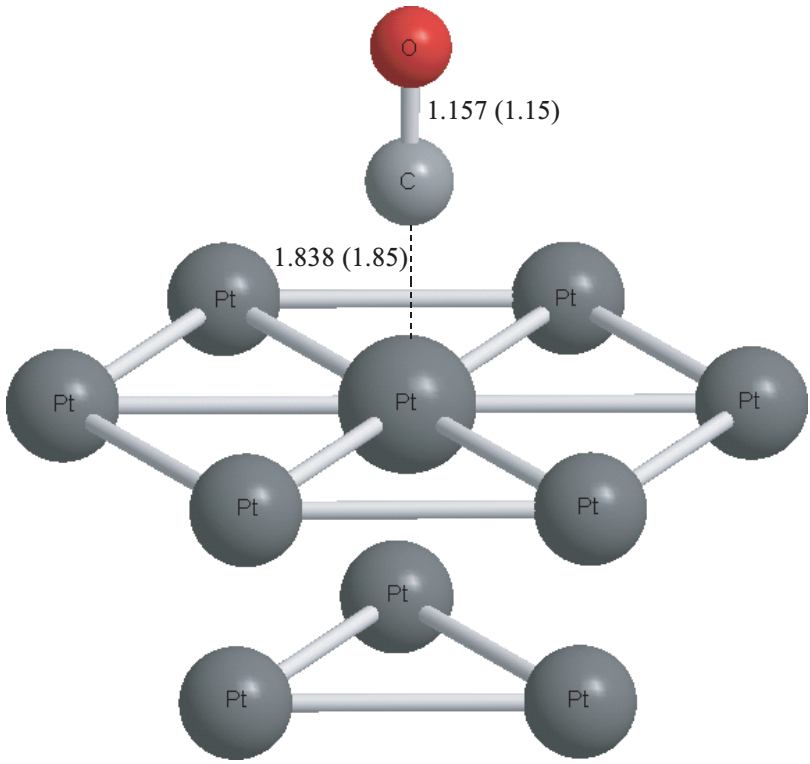

Fig. 1. The geometric structure of the CO molecule adsorbing Pt_{10} cluster that models the CO/Pt(111) system. Experimental values are in parentheses.[43]

The calculated structure of the CO molecule adsorbing the Pt_{10} cluster was in fair agreement with the experiment.[43] In this study, we paid attention to the $\sigma \rightarrow \pi^*$ and $\pi \rightarrow \pi^*$ excitations in CO and various excitations from the atop Pt to the π^* orbital of CO. The TDKS calculations were carried out on the GAMESS program[45] by using the BOP functional with Stevens–Krauss–Basch–Jasien (SKBJ) relativistic pseudopotentials plus a valence double-zeta basis set[46] for all constituent atoms. The point group C_{3v} symmetry of CO/Pt_{10} system was exploited in both KS and TDKS calculations. For threshold θ in Eq. (11), we examined four values; 10^{-1}, 5×10^{-2}, 10^{-2}, and 10^{-3}.

To explore the dominant configurations in TDKS excited states of small systems, we also calculated the vertical excitation energies of CO, H_2CO and C_6H_6 molecules. The geometrical structures of the molecules were set as the experimental ones. The TDKS calculations of the molecules were carried out on GAMESS using the BOP functional with the augmented Sadlej basis set.[47] The D_{2h} symmetry of C_6H_6 and the C_{2v} symmetry of CO and H_2CO were exploited. For those systems, we examined five thresholds; $\theta = 10^{-1}$, 5×10^{-2}, 10^{-2}, 5×10^{-3} and 10^{-3}.

4. Calculations

4.1. *CO/Pt_{10} system*

Table 1 summarizes the calculated vertical excitation energies of the intramolecular and metal-molecular transitions of the CO/Pt_{10} system for the SKBJ basis set for various threshold θ values in Eq. (11). "Full matrix" corresponds to the original TDKS result. Experimental singlet and triplet $\sigma \rightarrow \pi^*$ excitation energies of the CO molecule are 8.2 and 5.6 eV, respectively. Theoretical investigations of electronic excited states of admolecules on metal surfaces has become important because experiments on photochemistry are severely limited by small

Table 1. Calculated vertical excitation energies of CO/Pt_{10} system in eV using the SKBJ basis set.

Excitation	$\theta = 10^{-1}$	$\theta = 5 \times 10^{-2}$	$\theta = 10^{-2}$	$\theta = 10^{-3}$	Full Matrix
CO $\sigma \rightarrow \pi^*$ singlet	10.77	10.74	10.72	10.71	10.70
CO $\sigma \rightarrow \pi^*$ triplet	9.97	9.97	9.97	9.95	9.93
CO $\pi \rightarrow \pi^*$ singlet	9.87	9.87	9.87	9.86	9.86
CO $\pi \rightarrow \pi^*$ triplet	9.26	9.24	9.23	9.23	9.23
Pt $s\sigma \rightarrow$ CO π^* singlet	8.30	8.29	8.29	8.28	8.28
Pt $s\sigma \rightarrow$ CO π^* triplet	8.21	8.21	8.21	8.20	8.20
Pt $d\sigma \rightarrow$ CO π^* singlet	6.98	6.98	6.97	6.97	6.97
Pt $d\sigma \rightarrow$ CO π^* triplet	6.82	6.82	6.82	6.81	6.81
Pt $d\pi \rightarrow$ CO π^* singlet	7.43	7.43	7.43	7.43	7.43
Pt $d\pi \rightarrow$ CO π^* triplet	7.23	7.23	7.23	7.22	7.22
Pt $d\delta \rightarrow$ CO π^* singlet	7.13	7.13	7.13	7.12	7.12
Pt $d\delta \rightarrow$ CO π^* triplet	6.95	6.95	6.95	6.94	6.94

absorption cross-sections and short lifetimes of excited states.[34] It has been observed experimentally that excited states of admolecules frequently correlate with the states of metal surfaces and give broad resonances in absorption spectra.[48] However, experiments also suggested that there are excited states of admolecules that clearly exploit a characteristic in absorption spectra.[49,50] We therefore expect that the intramolecular and metal-molecular excitations may be described in practice with the configurations corresponding to the intramolecular or metal-admolecule transitions and other few transitions only. We should mention that the excitation energies obtained in this study may deviate considerably from the experimental values due to the low basis set quality, a cluster model that is not large enough for modeling a metal surface, or a poor description of the charge transfer excitation by TDKS specifically in metal-admolecule excitations. However, this calculation may be appropriate for investigating the electron configurations that are dominating intramolecular and metal-admolecule excitations of an admolecule on metal surface in TDKS calculation. As the tables indicate, the contracted TDKS precisely reproduces the vertical excitation energies of the original TDKS calculation within an error of 0.07 eV independent of the character of transition or the size of threshold θ. The decrease in calculated excitation energies as the threshold tightens corresponds to the stabilization of the calculated excited states due to the increase in number of electron configurations that are used to describe a single excitation. Using $\theta = 10^{-1}$ and 5×10^{-2}, we obtain excitation energies close to the original ones at almost the same level as those of $\theta = 10^{-2}$ and $\theta = 10^{-3}$ within errors of 0.07 and 0.04 eV, respectively. We should also emphasize that this contracted TDKS calculation always provides correct excitation energies close to the original TDKS results, independent of the differences in excitation character.

Table 2 displays the ranks of M_{qq^0} submatrices in Eq. (3) that are reduced by the present contraction scheme with thresholds of 10^{-1}, 5×10^{-2}, 10^{-2} and 10^{-3} (See Sec. 2). As found in the tables, the rank of submatrix for obtaining the intramolecular excitations of CO molecule decrease to less than 1/30 and 1/50 of the rank of the original TDKS matrix for $\theta = 5 \times 10^{-2}$ and 10^{-1}, respectively; the rank, e.g. in the $\pi \rightarrow \pi^*$ singlet excitation, is reduced from 10,901 to 296 for $\theta = 5 \times 10^{-2}$ and 157 for $\theta = 10^{-1}$. The rank of submatrix for obtaining the metal-admolecule excitations decreases to less than 1/40 and 1/80 of the rank of the original TDKS matrix for $\theta = 5 \times 10^{-2}$ and 10^{-1}, respectively. These results indicate that the low-lying intramolecular and metal-admolecule excitations of the CO/Pt_{10} system may be determined in practice by at most 1/30 of all of the electron configurations. However, it should be noted that the basis set is of double-zeta with no polarization or diffuse quality, which is not sufficiently accurate for calculating an excited state. We may therefore expect that the accuracy of the contracted TDKS for this system changes on the threshold θ by using a more accurate basis set. Nevertheless, we may say that in TDKS calculation only a small portion of electron configurations is necessary for quantitatively describing local excitations such as the present ones

Table 2. Ranks of M_{qq^0} submatrices in Eq. (3) after the contraction process with the thresholds θ of 10^{-1}, 5×10^{-2}, 10^{-2}, and 10^{-3} in Eq. (11), using the SKBJ basis set. Values in parentheses indicate the rank of the original TDKS matrix for each irrep.

Irrep	Excitation	Rank of Submatrix			
		$\theta = 10^{-1}$	$\theta = 5 \times 10^{-2}$	$\theta = 10^{-2}$	$\theta = 10^{-3}$
A_1 (10901)	CO $\pi \rightarrow \pi^*$ singlet	157	296	1269	6157
	CO $\pi \rightarrow \pi^*$ triplet	83	152	945	5834
	Pt $d\pi \rightarrow$ CO π^* singlet	179	316	1273	5954
	Pt $d\pi \rightarrow$ CO π^* triplet	89	177	726	5843
	Pt $d\delta \rightarrow$ CO π^* singlet	185	311	1204	5912
	Pt $d\delta \rightarrow$ CO π^* triplet	94	165	714	5842
E (9872)	CO $\sigma \rightarrow \pi^*$ singlet	86	181	990	5034
	CO $\sigma \rightarrow \pi^*$ triplet	58	110	793	4990
	Pt $d\sigma \rightarrow$ CO π^* singlet	123	243	902	4864
	Pt $d\sigma \rightarrow$ CO π^* triplet	63	121	548	4977
	Pt $s\sigma \rightarrow$ CO π^* singlet	106	198	978	4917
	Pt $s\sigma \rightarrow$ CO π^* triplet	50	103	677	4999

in which electron transitions within the admolecule or between the admolecule and a neighboring Pt atom are involved.

4.2. *Low-lying excitations of small prototype molecules*

To investigate the dominant configurations of excited states of molecules employing a high-quality basis set, we applied the contraction scheme to low-lying excitations of the three prototype molecules by using the augmented Sadlej basis set; CO, H_2CO, and C_6H_6 for thresholds of 10^{-1}, 5×10^{-2}, 10^{-2}, 5×10^{-3} and 10^{-3}. Tables 3 to 8 summarize the calculated vertical excitation energies and the ranks of M_{qq^0} submatrices. Experimental values of the corresponding excitation energies are also shown for comparison.

4.2.1. *CO molecule*

Table 3 displays low-lying excitation energies of carbon monoxide molecule obtained by using the present contraction scheme. The excitation energies given by the original TDKS calculation are also displayed. For comparison, corresponding experimental values[51] are also shown. As the table indicates, the contraction scheme reproduces the original TDKS excitation energies without significant loss of accuracy. The largest difference between the calculated values obtained with and without the contraction scheme was found in $^1\Pi$ valence excitation, with the errors of 0.24 and 0.21 eV with $\theta = 10^{-1}$ and 5×10^{-2}, respectively. For thresholds of 10^{-2} and smaller, the deviation from the original TDKS is within 0.06 eV. It is also found that the valence excitation energies of $^1\Delta$, $^1\Sigma^-$ and $^3\Sigma^-$ are almost completely reproduced even with $\theta = 10^{-1}$. Table 4 shows the ranks of M_{qq^0} submatrices for each of the thresholds. We may say that the numbers of electron configurations that

Table 3. Calculated vertical excitation energies of carbon monoxide molecule in eV using the augmented Sadlej basis set.

Excitation	$\theta = 10^{-1}$	$\theta = 5 \times 10^{-2}$	$\theta = 10^{-2}$	$\theta = 5 \times 10^{-3}$	$\theta = 10^{-3}$	Full Matrix	Exp[a]
Valence excitation							
$^1\Delta$	10.03	10.03	10.03	10.02	10.02	10.02	10.23
$^1\Sigma^-$	9.78	9.78	9.78	9.78	9.78	9.78	9.88
$^1\Pi$	8.49	8.46	8.31	8.28	8.26	8.25	8.51
$^3\Sigma^-$	9.78	9.78	9.78	9.78	9.78	9.78	9.88
$^3\Delta$	8.88	8.85	8.79	8.78	8.78	8.78	9.36
$^3\Sigma^+$	8.33	8.29	8.16	8.15	8.15	8.14	8.51
$^3\Pi$	6.04	6.01	5.94	5.94	5.94	5.94	6.32
Rydberg excitation							
$^1\Sigma^+$	9.48	9.46	9.45	9.45	9.45	9.45	12.4
$^1\Pi$	9.43	9.42	9.41	9.41	9.41	9.41	11.53
$^1\Sigma^+$	9.24	9.23	9.23	9.23	9.23	9.23	11.40
$^1\Sigma^+$	8.87	8.86	8.85	8.85	8.85	8.85	10.78
$^3\Pi$	9.35	9.34	9.34	9.34	9.34	9.34	11.55
$^3\Sigma^+$	9.20	9.20	9.20	9.20	9.20	9.20	11.3
$^3\Sigma^+$	8.72	8.71	8.71	8.71	8.71	8.71	10.4

[a]From Adamo *et al.*[51]

are dominant in $^1\Delta$, $^1\Sigma^-$, $^1\Pi$, $^3\Sigma^-$, $^3\Delta$, $^3\Sigma^+$ and $^3\Pi$ valence excitations correspond to the ranks of the submatrix with $\theta = 10^{-1}$, i.e. 14, 3, 2, 2, 4, 4 and 2, respectively. Comparing the solution vector of the original TDKS and that with $\theta = 10^{-1}$ in each of the valence excitations, we have found that the constituent electron configurations with weight (square of the coefficient) > 0.01 are similar. We have also found that all of the Rydberg excitation energies considered are reproduced essentially with threshold of 10^{-1}, although they are severely underestimated by the original TDKS calculation, as was found earlier.[16–19] This result may correspond to the fact that Rydberg excitations are in general of single-configuration character. Actually, the number of dominant configurations in each of the Rydberg excitations is estimated to be on the order of 10^0, as is shown in Table 4.

4.2.2. *H_2CO molecule*

The excitation energies of formaldehyde molecule obtained by the contraction scheme for each of the five thresholds and by the original TDKS calculation are displayed in Table 5. The experimental values[52,53] are also shown. As was found in the excitations of CO molecule, we found no significant deviation from the original TDKS of the excitation energies obtained by the contracted TDKS calculation. The largest deviation from the original TDKS calculation was found in $^1B_1$ ($\sigma \rightarrow \pi^*$) and $^3A_1$ ($\pi \rightarrow \pi^*$) excitations, with the deviations of 0.12 and 0.13 eV for $\theta = 10^{-1}$ and 0.10 and 0.10 eV for $\theta = 5 \times 10^{-2}$, respectively. For $\theta = 10^{-2}$ and smaller, the contracted TDKS reproduces the original TDKS excitation energies for these excitations within the error of 0.03 eV. It is also found that $^1A_2$ and $^3A_2$ valence excitation energies are almost fully reproduced even with thresholds of 10^{-1} and

Table 4. Ranks of M_{qq^0} submatrices in Eq. (3) in calculations of the excitation energies of carbon monoxide molecule after the contraction process with the thresholds θ of 10^{-1}, 5×10^{-2}, 10^{-2}, 5×10^{-3}, and 10^{-3} in Eq. (11), using the augmented Sadlej basis set. The rank of the original TDKS matrix for each irrep is also displayed for comparison.

Excitation	Rank of Submatrix					Full Matrix[a]
	$\theta = 10^{-1}$	$\theta = 5 \times 10^{-2}$	$\theta = 10^{-2}$	$\theta = 5 \times 10^{-3}$	$\theta = 10^{-3}$	
Valence excitation						
$^1\Delta$	14	30	87	103	137	201(A_1)
$^1\Sigma^-$	3	4	8	27	44	61(A_2)
$^1\Pi$	2	3	26	44	79	107(B_1, B_2)
$^3\Sigma^-$	2	6	30	38	45	61(A_2)
$^3\Delta$	4	14	89	106	137	201(A_1)
$^3\Sigma^+$	4	14	89	106	137	201(A_1)
$^3\Pi$	2	4	50	66	86	107(B_1, B_2)
Rydberg excitation						
$^1\Sigma^+$	6	25	83	100	137	201(A_1)
$^1\Pi$	3	5	27	48	79	107(B_1, B_2)
$^1\Sigma^+$	6	21	83	100	137	201(A_1)
$^1\Sigma^+$	4	20	83	100	137	201(A_1)
$^3\Pi$	3	8	58	72	86	107(B_1, B_2)
$^3\Sigma^+$	6	18	91	106	137	201(A_1)
$^3\Sigma^+$	4	14	89	106	137	201(A_1)

[a]The full matrix are reduced by using the C_{2v} symmetry. The corresponding irreps are in parentheses.

Table 5. Calculated vertical excitation energies of formaldehyde molecule in eV using the augmented Sadlej basis set.

Excitation	$\theta = 10^{-1}$	$\theta = 5 \times 10^{-2}$	$\theta = 10^{-2}$	$\theta = 5 \times 10^{-3}$	$\theta = 10^{-3}$	Full Matrix	Exp[a]
Valence excitation							
$^1B_1$ ($\sigma \rightarrow \pi^*$)	8.96	8.94	8.87	8.86	8.84	8.84	8.68
$^1A_2$ ($n \rightarrow \pi^*$)	3.88	3.88	3.87	3.86	3.86	3.86	3.94
$^3A_1$ ($\pi \rightarrow \pi^*$)	6.05	6.02	5.93	5.93	5.92	5.92	5.53
$^3A_2$ ($n \rightarrow \pi^*$)	3.23	3.23	3.20	3.20	3.20	3.20	3.50
Rydberg excitation							
$^1A_2$ ($n \rightarrow 3db_1$)	6.95	6.95	6.95	6.95	6.95	6.95	9.22
$^1A_2$ ($n \rightarrow 3pb_1$)	6.44	6.44	6.44	6.44	6.44	6.44	8.38
$^1B_2$ ($n \rightarrow 3pa_1$)	6.22	6.22	6.21	6.21	6.21	6.21	8.12
$^1A_1$ ($n \rightarrow 3pb_2$)	6.27	6.27	6.27	6.27	6.27	6.27	7.97
$^1B_2$ ($n \rightarrow 3sa_1$)	5.66	5.66	5.65	5.65	5.65	5.65	7.09
$^3B_2$ ($n \rightarrow 3pa_1$)	6.19	6.19	6.19	6.19	6.19	6.19	7.96
$^3A_1$ ($n \rightarrow 3pb_2$)	6.22	6.22	6.22	6.22	6.22	6.22	7.79
$^3B_2$ ($n \rightarrow 3sa_1$)	5.57	5.57	5.56	5.56	5.56	5.56	6.83

[a]From Haddad *et al.*[52] and Foresman *et al.*[53]

5×10^{-2}. The ranks of M_{qq^0} submatrices for each of the thresholds are displayed in Table 6. Considerable decrease in deviation of $^1B_1$ and $^3A_1$ valence excitation energies with θ changing from 5×10^{-2} to 10^{-2} may correspond to the considerable increase in rank of the submatrix, as is shown in the table. As we indicated

Table 6. Ranks of M_{qq^0} submatrices in Eq. (3) in calculations of the excitation energies of formaldehyde molecule after the contraction process with the thresholds θ of 10^{-1}, 5×10^{-2}, 10^{-2}, 5×10^{-3}, and 10^{-3} in Eq. (11), using the augmented Sadlej basis set. The rank of the original TDKS matrix for each irrep is also displayed for comparison.

Excitation	Rank of Submatrix					Full Matrix[a]
	$\theta = 10^{-1}$	$\theta = 5 \times 10^{-2}$	$\theta = 10^{-2}$	$\theta = 5 \times 10^{-3}$	$\theta = 10^{-3}$	
Valence excitation						
$^1B_1$ ($\sigma \rightarrow \pi^*$)	2	6	32	52	84	115
$^1A_2$ ($n \rightarrow \pi^*$)	1	2	12	35	55	78
$^3A_1$ ($\pi \rightarrow \pi^*$)	2	14	120	137	164	227
$^3A_2$ ($n \rightarrow \pi^*$)	3	4	45	52	55	78
Rydberg excitation						
$^1A_2$ ($n \rightarrow 3db_1$)	1	4	15	35	55	78
$^1A_2$ ($n \rightarrow 3pb_1$)	1	4	14	35	55	78
$^1B_2$ ($n \rightarrow 3pa_1$)	2	3	47	76	121	164
$^1A_1$ ($n \rightarrow 3pb_2$)	8	23	94	123	168	227
$^1B_2$ ($n \rightarrow 3sa_1$)	1	2	44	74	121	164
$^3B_2$ ($n \rightarrow 3pa_1$)	3	7	97	114	131	164
$^3A_1$ ($n \rightarrow 3pb_2$)	2	15	120	137	164	227
$^3B_2$ ($n \rightarrow 3sa_2$)	1	5	97	113	131	164

[a]The full matrix are reduced by using the C_{2v} symmetry. The corresponding irreps are in parentheses.

in the excitation of CO molecule, it is presumed from the ranks of submatrices with $\theta = 10^{-1}$ that the numbers of electron configurations that essentially dominate the $^1B_1$, $^1A_2$, $^3A_1$ and $^3A_2$ valence excitations are 2, 1, 2 and 3, respectively. Actually, comparing the solution vectors of the valence excitations with $\theta = 10^{-1}$ and those obtained by the original TDKS calculation, the dominant configurations (with square of coefficient > 0.01) in the solution vectors are found to be similar. For Rydberg excitations, all the excitation energies are reproduced even with $\theta = 10^{-1}$ within the deviation of 0.03 eV from the original TDKS. Table 6 indicates that the ranks of submatrices with $\theta = 10^{-1}$ are 1/25 less than those of the original TDKS calculation. This result is supported by the single-excitation character of Rydberg excitations. We should also mention that the ranks of submatrices of valence excitations with $\theta = 10^{-1}$ are on the same order as those of Rydberg excitations. It is therefore presumed that the low-lying excitations of H_2CO molecule considered may be substantially described with 1/25 of all of the electron configurations in TDKS calculation.

4.2.3. *C_6H_6 molecule*

Table 7 shows calculated low-lying excitation energies of benzene molecule for the five thresholds. Experimental values are also shown for comparison.[54] As contrasted to the CO and H_2CO calculations, it was found that much smaller threshold ($\theta = 10^{-2}$–10^{-3}) is required to reproduce the original TDKS results for valence

Table 7. Calculated vertical excitation energies of benzene molecule in eV using the augmented Sadlej basis set.

Excitation	$\theta = 10^{-1}$	$\theta = 5 \times 10^{-2}$	$\theta = 10^{-2}$	$\theta = 5 \times 10^{-3}$	$\theta = 10^{-3}$	Full Matrix	Exp[a]
Valence $\pi \rightarrow \pi^*$ excitation							
1^1E_{1u}	8.23	7.57	6.92	6.88	6.81	6.80	6.94
1^1B_{1u}	6.51	6.30	5.97	5.91	5.88	5.88	6.2
1^3B_{2u}	4.92	4.92	4.91	4.90	4.90	4.90	5.6
1^1B_{2u}	5.24	5.24	5.19	5.18	5.17	5.16	4.9
1^3E_{1u}	4.66	4.66	4.63	4.62	4.62	4.62	4.76
1^3B_{1u}	4.29	4.23	4.13	4.10	4.08	4.08	3.94
Rydberg $\pi \rightarrow \pi^*$ excitation							
2^1A_{1g}	6.75	6.74	6.72	6.72	6.72	6.72	7.81?
1^1E_{2g}	6.70	6.70	6.70	6.70	6.69	6.69	7.81
1^1A_{2g}	6.72	6.72	6.72	6.72	6.72	6.72	7.81
2^1E_{1u}	6.29	6.29	6.28	6.28	6.28	6.28	7.41
1^1E_{2u}	6.04	6.04	6.04	6.04	6.04	6.04	6.953
1^1A_{2u}	6.04	6.04	6.04	6.04	6.04	6.03	6.932
Rydberg $\pi \rightarrow \sigma^*$ excitation							
2^1E_{1g}	6.34	6.34	6.34	6.34	6.34	6.34	7.535
1^1B_{2g}	6.49	6.49	6.49	6.49	6.49	6.49	7.46
1^1B_{1g}	6.48	6.48	6.48	6.48	6.48	6.48	7.46
1^1E_{1g}	5.60	5.60	5.60	5.60	5.60	5.60	6.334

[a]From Paker *et al.*[54]

$\pi \rightarrow \pi^*$ excitations, while the original TDKS energies for Rydberg $\pi \rightarrow \pi^*$ and $\pi \rightarrow \sigma^*$ excitations were reproduced even with $\theta = 10^{-1}$. For the 1^1E_{1u} and 1^1B_{1u} valence excitations, the deviations from the original TDKS values are as large as 1.43 and 0.63 eV with $\theta = 10^{-1}$, and 0.77 and 0.42 eV with $\theta = 5 \times 10^{-2}$, respectively. For $\theta = 10^{-2}$, the contracted TDKS reproduces the valence $\pi \rightarrow \pi^*$ excitation energies within the error of 0.12 eV relative to the original TDKS. This tighter threshold required for reproducing the original TDKS result than that for CO and H_2CO molecules may correspond to the considerable multiconfiguration character of the valence excited states of C_6H_6 molecule due to the severe quasi-degeneracy. In *ab initio* wavefunction approach, 1^1E_{1u} and 1^1B_{1u} states are classified into the ionic plus states dominated by the single excitations, while 1^1B_{2u} into the covalent minus state which includes a large fraction of doubly excited configurations.[55] The table indicates that the excitation energy of 1^1B_{2u} state is almost fully reproduced even with $\theta = 10^{-1}$, in contrast to those of 1^1E_{1u} and 1^1B_{1u} states. We may therefore say that the double excitation is partly recovered by the dynamical correlation of the density functionals employed in TDKS calculations even though doubly excited configurations are not explicitly taken into account. In Table 8, the ranks of M_{qq^0} submatrices are also displayed for various thresholds. As the table indicates, the number of electron configurations that are incorporated in describing 1^1E_{1u} and 1^1B_{1u} valence excitations with $\theta = 10^{-1}$ and smaller is more than 1/6 of that of the original TDKS. This result may be consistent with the multiconfiguration character of these excitations. However, the number of dominant configurations indicated

Table 8. Ranks of M_{qq^0} submatrices in Eq. (3) in calculations of the excitation energies of benzene molecule after the contraction process with the thresholds θ of 10^{-1}, 5×10^{-2}, 10^{-2}, 5×10^{-3}, and 10^{-3} in Eq. (11), using the augmented Sadlej basis set. The rank of the original TDKS matrix for each irrep is also displayed for comparison.

Excitation	Rank of Submatrix					Full Matrix[a]
	$\theta = 10^{-1}$	$\theta = 5 \times 10^{-2}$	$\theta = 10^{-2}$	$\theta = 5 \times 10^{-3}$	$\theta = 10^{-3}$	
Valence $\pi \rightarrow \pi^*$ excitation						
1^1E_{1u}	3	13	130	228	414	$618(B_{3u})$, $660(B_{1u})$
1^1B_{1u}	3	13	130	228	414	$660(B_{1u})$
1^3B_{2u}	2	2	136	328	416	$618(B_{3u})$
1^1B_{2u}	2	3	94	173	354	$618(B_{3u})$
1^3E_{1u}	2	3	187	362	441	$618(B_{3u})$, $660(B_{1u})$
1^3B_{1u}	2	3	187	362	441	$660(B_{1u})$
Rydberg $\pi \rightarrow \pi^*$ excitation						
2^1A_{1g}	6	15	149	251	431	$661(A_g)$
1^1A_{2g}	4	8	71	130	345	$617(B_{2g})$
1^1E_{2g}	6	15	149	251	431	$617(B_{2g})$, $661(A_g)$
2^1E_{1u}	4	10	126	221	411	$618(B_{3u})$, $660(B_{1u})$
1^1E_{2u}	6	9	43	89	227	$327(A_u)$, $357(B_{2u})$
1^1A_{2u}	6	9	43	89	227	$357(B_{2u})$
Rydberg $\pi \rightarrow \sigma^*$ excitation						
2^1E_{1g}	2	7	35	77	221	$358(B_{3g})$, $329(B_{1g})$
1^1B_{2g}	4	7	35	79	221	$358(B_{3g})$
1^1B_{1g}	4	7	23	62	203	$329(B_{1g})$
1^1E_{1g}	1	4	30	76	221	$358(B_{3g})$, $329(B_{1g})$

[a]The full matrix are reduced by using the D_{2h} symmetry. The corresponding irreps are in parentheses.

above is intuitively large. It is expected that the dominant configurations may be picked up more correctly by applying the contraction scheme for various θ's between 10^{-2} and 5×10^{-3}. The electron configurations of benzene are probably coupled with various degrees. In contrast to the calculations of CO and H_2CO molecules, the dominant configurations with weight > 0.01 in calculations of 1^1E_{1u} and 1^1B_{1u} valence excitations with $\theta = 10^{-1}$ are found to be different from the counterpart in the original TDKS. It was also found that the corresponding triplet excitation energies are estimated correctly even with $\theta = 10^{-1}$ or 5×10^{-2}, in contrast to the singlet ones. This result indicates that the near-degeneracy does not influence the triplet excitations as severely as the singlet counterpart in TDKS calculations. For Rydberg excitations, the table indicates that the number of ranks required for reproducing the original TDKS values is on the order of 10^0, as was found for Rydberg excitations of CO and H_2CO molecules.

5. Conclusions

We have investigated the electron configurations that are dominant in describing an excited state in time-dependent Kohn–Sham (TDKS) calculation on the basis

of the argument by Appel *et al.*[31] By making use of their approach, transitions that contribute to the excitation energy of a transition of interest are picked up by imposing the condition of Eq. (11) containing only the diagonal elements of the matrix M in Eq. (3) and the energy gaps of KS orbitals. By calculating only the submatrix that is contracted for the collected transitions, we can obtain the corresponding excitation energy which approximates the original full TDKS excitation energy. The efficiency and the accuracy of this contracted TDKS calculation depends on threshold θ of Eq. (11), which determines if an electron configuration energetically contributes to the calculated TDKS excitation energy of an electron transition of interest. We can pick up electron configurations that are dominant in excited states of interest by applying this contracted TDKS to calculations of excitation energies for various θ's.

This contracted TDKS was first applied to the calculation of the excitation energies of a CO molecule adsorbing Pt_{10} cluster. Calculated results of the CO/Pt_{10} system showed that the TDKS calculation employing the contracted matrix reproduced the low-lying excitation energies of the original TDKS calculation within an error of 0.07 eV independent of the character of excitation. In the intramolecular excitations of CO molecule such as the $\pi \rightarrow \pi^*$ and $\sigma \rightarrow \pi^*$ excitations, the number of electron configurations required in practice to reproduce the original TDKS result was estimated to be less than 1/30 of that of the original full TDKS. In the metal-admolecule excitations, it was found to be less than 1/40 of that of the original full TDKS. It should be mentioned that the accuracy of the contracted TDKS for this system may change by using a more accurate basis set than the present one (double-zeta plus no polarization or diffusion). However, we may say that the excitations of this system that we found to be dominated by a small portion of all of the electron configurations is attributed to the locality of the excitations, in which the admolecule and a neighboring Pt atom are involved.

For investigating the dominant electron configurations in excited states described by the TDKS employing a high-quality basis set, we applied the present contraction scheme to low-lying excitations of CO, H_2CO, and C_6H_6 molecules by using the augmented Sadlej basis set. It has been found that the low-lying valence excitations of CO and H_2CO molecules may be substantially dominated by a few configurations in TDKS calculation, within the deviations of the calculated excitation energies from the original TDKS of 0.24 eV and 0.13 eV, respectively. On the other hand, we found that relatively large number of electron configurations are required to give accurate valence excitations of benzene, because there are many configurations that are significantly coupled with various degrees due to the severe quasi-degeneracy of this molecule. We also found that the double excitation may be partly recovered by the dynamical correlation of the functionals used, as was indicated previously.[5]

These results indicate that the accuracy and the efficiency of the present TDKS in describing electronic excitations is severely influenced by the degeneracy of the

system. This situation may correspond to the applicability of a excitation theory which is based on a single-reference wavefunction. Nevertheless, we have confirmed that the present TDKS can describe low-lying excited states of molecules by incorporating only a small portion of all of the electron configurations. In actual computations, this finding may be made use of as the preprocessing for solving eigenvalue problems by the Davidson's iterative subspace method, e.g. efficient setup of the initial guess of trial vector, which contributes to the rapid convergence of the diagonalization. This may also accelerate the TDKS process involving successive calculations of specific excited states, such as the potential energy surface calculation and the subsequent excited state molecular dynamics simulation. Such an investigation is in progress.

Acknowledgments

We are very grateful to Professor N. C. Handy for his helpful advices about coding the TDKS program. This research was supported by a Grant-in-Aid for Scientific Research on a Priority Area (A) and for the Encouragement of Young Scientists (T. Tsuneda) from the Japanese Ministry of Education, Science, Sports, and Culture and by a grant from the Genesis Research Institute, Inc.

References

1. Gross EKU, Kohn W, *Adv Quant Chem* **21**:255, 1990.
2. Casida ME, in Chong DP (ed.), *Recent Advances in Density Functional Methods, Part I*, World Scientific, Singapore, 1995.
3. Petersilka M, Gossmann UJ, Gross EKU, *Phys Rev Lett* **76**:1212, 1999.
4. Bauernschmitt R, Ahlrichs R, *Chem Phys Lett* **256**:454, 1996.
5. Hirata S, Head–Gordon M, *Chem Phys Lett* **302**:375, 1999.
6. Guan J, Casida ME, Salahub DR, *J Mol Struct* THEOCHEM **527**:229, 2000.
7. Dai B, Deng K, Yang J, Zhu Q, *J Chem Phys* **118**:9608, 2003.
8. Broclawik E, Borowski T, *Chem Phys Lett* **339**:433, 2001.
9. Dai B, Deng K, Yang J, *Chem Phys Lett* **364**:188, 2002.
10. Rosa A, Baerends EJ, van Gisbergen SJA, van Lenthe E, Groeneveld JA, Snijders JG, *J Am Chem Soc* **121**:10356, 1999.
11. Adamo C, Scuseria GE, Barone V, *J Chem Phys* **111**:2889, 1999.
12. van Gisbergen SJA, Rosa A, Ricciardi G, Baerends EJ, *J Chem Phys* **111**:2499, 1999.
13. Yamaguchi Y, *J Chem Phys* **117**:9688, 2002.
14. Hirata S, Lee T, Head–Gordon M, *J Chem Phys* **111**:8904, 1999.
15. Hirata S, Head–Gordon M, Szczepanski J, Vala M, *J Phys Chem A* **107**:4940, 2003.
16. Casida ME, Jamorski C, Casida KC, Salahub DR, *J Chem Phys* **108**:4439, 1998.
17. Tozer DJ, Handy NC, *J Chem Phys* **109**:10180, 1998.
18. Schipper PRT, Gritsenko OV, van Gisbergen SJA, Baerends EJ, *J Chem Phys* **112**:1344, 2000.
19. Grüning M, Gritsenko OV, van Gisbergen SJA, Baerends EJ, *J Chem Phys* **114**:652, 2001.
20. Dreuw A, Weisman JL, Head–Gordon M, *J Chem Phys* **119**:2943, 2003.
21. Diedrich C, Grimme S, *J Phys Chem* **107**:2524, 2003.

22. Grimme S, Parac M, *Chem Phys Chem* **3**:292, 2003.
23. Casida ME, Gutierrez F, Guan J, Gadea F-X, Salahub D, Daudey J-P, *J Chem Phys* **113**:7062, 2000.
24. Furche F, Ahlrichs R, *J Chem Phys* **117**:7433, 2002.
25. Caillie CV, Amos RD, *Chem Phys Lett* **317**:159, 2000.
26. Caillie CV, Amos RD, *Chem Phys Lett* **308**:249, 1999.
27. Davidson ER, *J Comput Phys* **17**:87, 1975.
28. Bauernschmitt R, Häser M, Treutler O, Ahlrichs R, *Chem Phys Lett* **264**:573, 1997.
29. Stratmann RE, Scuseria GE, Frisch MJ, *J Chem Phys* **109**:8218, 1998.
30. Hirata S, Head–Gordon M, Bartlett RJ, *J Chem Phys* **111**:10774, 1999.
31. Appel H, Gross EKU, Burke K, *Phys Rev Lett* **90**:043005, 2003.
32. Casida ME, in Seminario JM (ed.), *Recent Developments and Applications in Density-Functional Theory*, pp. 155, Elsevier, Amsterdam, 1996.
33. Swain S, *Adv At Mol Phys* **22**:387, 1982.
34. Buenker RJ, Liebermann H-P, Whitten JL, *Chem Phys* **265**:1, 2001, and references therein.
35. Nakatsuji H, Morita H, Nakai H, Murata Y, Fukutani K, *J Chem Phys* **104**:714, 1996.
36. For more details about $DMol^3$, see http://www.accelrys.com/mstudio/dmol3.html.
37. Delley BJ, *Chem Phys* **92**:508, 1990.
38. Delley BJ, *Phys Chem* **100**:6107, 1996.
39. Delley B, *Int J Quant Chem* **69**:423, 1988.
40. Delley BJ, *Chem Phys* **113**:7756, 2000.
41. Becke AD, *Phys Rev A* **38**:3098, 1988.
42. Tsuneda T, Suzumura T, Hirao K, *J Chem Phys* **110**:10664, 1999.
43. Ogletree DF, VanHove MA, Somorjai GA, *Surf Sci* **173**:351, 1986.
44. Gil A, Clotet A, Ricart JM, Kresse G, Hernández MG, Rösch N, Sautet P, *Surf Sci* **530**:71, 2003.
45. http://www.msg.ameslab.gov/GAMESS/GAMESS.html.
46. Stevens WJ, Basch H, Krauss M, *J Chem Phys* **81**:6026, 1984; Stevens WJ, Krauss M, Basch H, Jasien PG, *Can J Chem* **70**:612, 1992.
47. Sadlej AJ, *Collec Czech Chem Commun* **53**:1995, 1988; *Theor Chim Acta* **79**:123, 1992.
48. Ho W, in Betz G, Varga P (eds.), *Desorption Induced by Electronic Transitions*, pp. 48, Springer, New York, 1990.
49. Zhou X-L, White JM, *Adv Ser Phys Chem* **5**:1141, 1995.
50. Harrison I, in Dai H-L, Ho W (eds.), *Laser Spectroscopy and Photochemistry on Metal Surfaces*, World Scientific, Singapore, 1995.
51. Adamo C, Scuseria GE, Barone V, *J Chem Phys* **111**:2889, 1999 and references therein.
52. Haddad CM, Foresman JB, Wiberg KB, *J Phys Chem* **97**:4293, 1993.
53. Foresman JB, Head–Gordon M, Pople JA, Frisch MJ, *J Phys Chem* **96**:135, 1992.
54. Paker MJ, Dalskov EK, Enevoldsen T, Jensen HJA, Oddershede J, *J Chem Phys* **105**:5886, 1996.
55. Hashimoto T, Nakano H, Hirao K, *J Mol Struct THEOCHEM* **451**:25, 1998.